Dynamics of a Duffing Oscililator System

Jongoh (Andy) Jeong
Professor Anita Raja
Ph235 Physics Simulations
29 April 2019

Abstract
The chaotic behavior in motion is not unusual to observe in practice in common nonlinear differential equations. Through close examination of nonlinear dynamics of a system governed by a Duffing's Equation, one can observe how phase-space motion follows a strange attractor as harmonic excitations are applied to the system. A Duffing oscillator system of complexity as simple as a second-order ordinary differential equation exhibits bifurcation past some threshold value of excitation due to periodic doubling, bounded by five parameters and initial conditions. Through visual aids and graphical responses, the chaotic motion of a Duffing system (i.e. spring) is observed, and verified in simple visualization techniques in Python.

Introduction

Initially, the objective of this project was to demonstrate a nonlinear dynamic system whose motion is governed by the Duffing's Equation through specific application of a magnetoelastic steel beam structure that is deflected by two magnets and under external excitation force at some frequency, the structure known as a 'Moonbeam.' However, due to limited time and understanding of resources on mathematical motions and its specific physical dynamics involving multiple factors including gravity, friction, elasticity of the beam and magnetic forces acting on the system altogether, it was deemed not feasible for the time being.

The approach is thus revised to explore and demonstrate chaotic motions given various parameters and initial conditions, identify the point of bifurcation and enhance understanding of a Duffing Oscillator through visualizations. The numerical approximation to solve for the variables would involve Runge-Kutta method, and thus would carry an error of order 5. In analyzing the behavior of the system from multiple perspectives, topics including numerical approximation of a nonlinear ordinary differential equation using RK4, visualization of time and spatial data as well as Poincare sections for chaos and animation would pertain to the course materials closely.

Duffing Oscillator (Equation)

Duffing Equation, first developed by a German engineer and researcher Georg Wilhelm Christian Casper Duffing (1861-1944), is a term for almost any dynamical system with periodic forcing and nonlinear elasticity, which exhibits chaos under certain parameters; it can also have a damping coefficient. It is nowadays more commonly used to describe an oscillator with a cubic stiffness term, regardless of presence of damping or excitation.

$$\mathrm{m}\frac{d^2x}{dt^2} + \delta\frac{dx}{dt} + \alpha x + \beta x^3 = F(t)$$

Equation 1. Duffing Equation

Each term represents the inertia of the mass, damping coefficient, spring force coefficient (linear stiffness), nonlinearity, and excitation force, respectively, where damping allows for dissipation of energy and forcing function F(t) restores the energy dissipated from it on the other hand. Eq. 1 exhibits chaotic behavior for $\alpha > 0$, and it can be interpreted as a forced oscillator with a spring whose restoring force is $F_s = -\alpha x - \beta x^3$. For β>0, the system can be represented as a "hard spring," and for β<0, "soft spring." For α<0 (purely imaginary), the Duffing oscillator could model dynamics of a point mass in a double-well potential, and can be interpreted as a magnetoelastic steel beam moving periodically between two magnets by deflection and excitation force, whereby chaotic motion is observed.

A resonance phenomenon is defined for a conservative oscillator (force=0), or a dissipative oscillator (force>0) as a noticeable increase in the amplitude of oscillations near certain forcing frequencies. The cubic nonlinear term, giving rise to amplitude dependent natural frequency, causes the system to exhibit more resonances in addition to the main harmonic resonance.

Throughout the analysis, there are a few assumptions with regards to external parameters acting on the system.

1) The resistance proportional to velocity neglected.
2) Gravitational acceleration and other external forces are neglected other than specified excitation F(t). F(t) is assumed to be of form $\gamma cos(\omega t)$.
3) Mass is assumed to be a unit mass (1kg) for simplicity.

With the above assumptions, the energy E(t) can be calculated as follows.

$$F_{net} = \mathrm{m}\ddot{x} = -\delta\dot{x} - \alpha x - \beta x^3 + \gamma\cos(\omega t)$$

- Potential Energy $PE = -\int F_{net}$

$$= -\int \mathrm{m}\left(-\delta\dot{x} - \alpha x - \beta x^3 + \gamma\cos(\omega t)\right)dx$$

$$= \mathrm{m}\left(\delta\dot{x}\dot{x} + \frac{\alpha}{2}x^2 + \frac{\beta}{4}x^4 - \gamma\cos(\omega t)\right)$$

- Potential V $= \frac{PE}{m} = \delta\dot{x}\dot{x} + \frac{\alpha}{2}x^2 + \frac{\beta}{4}x^4 - \gamma\cos(\omega t)$

- Kinetic Energy KE $= \frac{1}{2}m\dot{x}^2$

- Total Energy (Hamiltonian) = E = PE + KE

The total sum of potential and kinetic energy associated with the system, or Hamiltonian, is expected to be conserved (constant) throughout the iterations of time and space.

Stability and Eigenvalues of Jacobian Matrix

Assuming friction due to velocity is neglected, the equation for total energy in free motion ($\delta = 0, \gamma = 0$) can be integrated over time by multiplying by the first derivative of x as follows[9]:

$$\dot{x}(\ddot{x} + \alpha x + \beta x^3) = \frac{d}{dt}\left(\frac{1}{2}\dot{x} + \frac{1}{2}\alpha x^2 + \frac{1}{4}\beta x^4\right) = \frac{d}{dt}(H) = 0$$

$$Integrating, \qquad E(t) = \frac{1}{2}\dot{x}^2 + \frac{1}{2}\alpha x^2 + \frac{\beta}{4}x^4 = \text{constant}$$

where H is the Hamiltonian for the free motion Duffing equation.

For $\alpha, \beta > 0$, the solution to the equation has bounds

$$|x| \leq \sqrt{\frac{2H}{\alpha}}, |\dot{x}| \leq \sqrt{2H}.$$

With damping in effect ($\delta \geq 0$), $\frac{dE(t)}{dt} = -\delta\dot{x}^2 \leq 0$. This implies that $E(t)$ is locally asymptotically stable about the origin; in other words, it is a Lyapunov function. A Lyapunov function is defined as a function that is locally positive definite, and its time derivative is locally negatively definite. In this case, the total conservative energy E(t) > 0, and $\dot{E}(t) < 0 \; \forall \; t >$ 0. From this observation, one can deduce that the equilibrium point of this function is Lyapunov stable.

For nonzero $\alpha, \beta \; coefficients,$

$solutions \; to \; the \; equations \; can \; be \; determined$

$from \; a \; simple \; cubic \; equation$

$$\alpha x + \beta x^3 = \mathrm{x}(\alpha + \beta x^2) = 0,$$

$$\text{thus x} = \pm\sqrt{-\frac{\alpha^2}{\beta}} \left(for \; \frac{\alpha^2}{\beta} < 0\right) \; and \; x = 0.$$

In order to understand the stability at these points of equilibrium, Eq. 1 can be written as two first derivative equations[7, 8].

$$\frac{\mathrm{d}}{\mathrm{dt}}\begin{pmatrix} x \\ \dot{x} \end{pmatrix} = \begin{pmatrix} \dot{x} \\ -\delta\dot{x} - x - \beta x^3 \end{pmatrix},$$

and the Jacobian matrix

$$J(x) = \begin{pmatrix} 0 & 1 \\ -\alpha - 3\beta x^2 & -\delta \end{pmatrix} for \; \alpha, \beta, \delta > 0$$

Examining the eigenvalues of the Jacobian matrix, one can determine the stability of the system at the fixed point.

$at \; fixed \; point \; x = 0,$

Stable equilibrium for $\alpha \geq 0$,

$$\because \prec_{eig} = \frac{-\delta \pm \sqrt{\delta^2 - 4\alpha}}{2} > 0,$$

$at \; fixed \; point \; x = \pm\sqrt{-\frac{\alpha^2}{\beta}},$

unstable equilibrium for $\delta, \alpha > 0$,

$$\because \prec_{eig} = \frac{-\delta \pm \sqrt{\delta^2 + 8\alpha}}{2} < 0$$

Lyapunov Exponents (for unforced Duffing equation)

The purpose of Lyapunov exponents is to determine the rate of growth of distance between neighboring trajectories and check for stability of the system. It is estimated, for trajectory x(t) and time t, to be

$$\prec \cong \frac{1}{\mathrm{t}}\ln\frac{\|\delta x(t)\|}{\|\delta x(0)\|}.$$

However, for infinitesimal δx, the Jacobian matrix is by definition,

$$J_{ij}(x_0) = \lim_{\delta \mathrm{x}(0)\to 0}\frac{\delta x_i(t)}{\delta x_j(0)} = \frac{\delta x_i(t)}{\delta x_j(0)},$$

thus the Lyapunov exponent can be computed from the linearization:

$$\prec_{LE}(x_0) = \lim_{t\to\infty}\frac{1}{t}\ln\left\|\frac{J(x_0)\delta x_0}{\delta x_0}\right\| = \lim_{t\to\infty}\frac{1}{2t}\ln(\hat{n}^T J^T J\hat{n}),$$

where $\hat{n} = \frac{\delta x_0}{\|\delta x_0\|}$ $(initial \; orientation \; unit \; vector)$.

Eventually, the leading exponent becomes

$$\prec_{leading \; LE}(x_0) = \lim_{t\to\infty}\frac{1}{t}\ln\left|\prec_{eig,Jacobian}\right|,$$

While there exist a number of well known algorithms to calculate the Lyapunov exponents such as Wolf's Algorithm, these make use of systems that involve 2 or more variables in the systems; for this particular ordinary differential equation with single variable x, approximation using eigenvalues of the 2-by-2 Jacobian matrix suffice to measure stability of the system[12].

Approach to numerical approx. using RK4

The basis for determining chaos in any nonlinear dynamics given a set of parameters and initial conditions is the correct approximation of the positional components. For Duffing Oscillator – second-order ordinary differential equation – it was

relatively easier than other systems like Rossler attractor involving differentials in three dimensions. To apply 4th order Runge-Kutta algorithm, the initial equation (Eq. 1) is taken apart into three first-order equations; the angular frequency (third equation), however, is neglected as it is initially defined, with the assumption that the excitation has the form $\cos(\omega t + \theta)$.

$$\mathrm{m}\frac{d^2x}{dt^2} + \delta\frac{dx}{dt} + \alpha x + \beta x^3 = F(t)$$

$$\dot{x} = v$$
$$\dot{v} = -\delta v - \alpha x - \beta x^3$$
$$\dot{\theta} = w$$

Runge-Kutta method involves approximating derivates at a halfway point, as well as at each endpoints, such that it takes derivates at t_0 once, at $t_{h/2}$ twice (at different y-points), and at t_h once, each with different weights. By approximating each successive derivative from previously computed derivative and taking each computed value at its weight, the correctness at the step size increases. As the implementation itself may be little tricky and prone to error, verification process is performed by estimating the value at the identical time point, with the step size halved each time. Then the error ratio of each value compared to a "true" value is computed, and checked that the error ratio converges to ~16, which is the order of RK4 accuracy as expected[1].

Compared to Euler's Method, Newton's Method, or other numerical approximation methods for nonlinear differential equations, Runge-Kutta method poses advantage in accuracy and error bounds. While performing fewer computations, it, on the other hand, achieves to yield a reasonable solution to the accuracy much better than that of Euler's. By using linear combinations of f(x,t) to approximate y(t), it closely matches up with Taylor series approximation, which tends to the exact solution in general.

Table 1 Fourth-order Runge-Kutta Implementation Verification[1]

Step size (h)	Approximation of x at t = 0.1, x_{approx}	Final Global Error(F.G.E) at t = 0.1 (x_{approx}- x_{true})	Error Ratio
0.1	-0.0018921715207243900	-0.0000000076565361900	-
0.05	-0.0018921642988212700	-0.0000000004346330700	17.6
0.025	-0.0018921638899839600	-0.0000000000257957601	16.8
0.0125	-0.0018921638657577500	-0.0000000000015695500	16.4
0.0001	-0.0018921638641882000 (=x_{true})	(assume true value)	-

Results – phase space diagram

A bifurcation point is the point where the change in the parameter values results in a change in the stability at the equilibrium point(s). This can be either experimentally observed from plotting displacement against time and comparing the periods as parameter values are changed, or determined from the eigenvalue of the Jacobian matrix, whereby a negative eigenvalue (purely imaginary) implies definite presence of bifurcation. At the point at which the period of the forcing is doubled, or the point of bifurcation, the phase space diagram no longer exhibits periodic or quasi-periodic behavior; rather, it has a chaotic motion, or a strange attractor, and the usual hysteresis loop is observed for the frequency response[8,10].

In order to observe the period doubling bifurcation effect as the ratio of amplitude of the excitation to the damping coefficient increases, the force is iterated from 0 to 0.6, by increments of h (step size). As experimentally observed, the ratio value of around 33.0 is determined to be the point of bifurcation, when the period doubling occurs.

The bifurcation figure below is drawn with the parameters:

Initial conditions : x=0, v=0

δ = 0.01, α = 1, β = 1, w = 1.414, h = 0.01

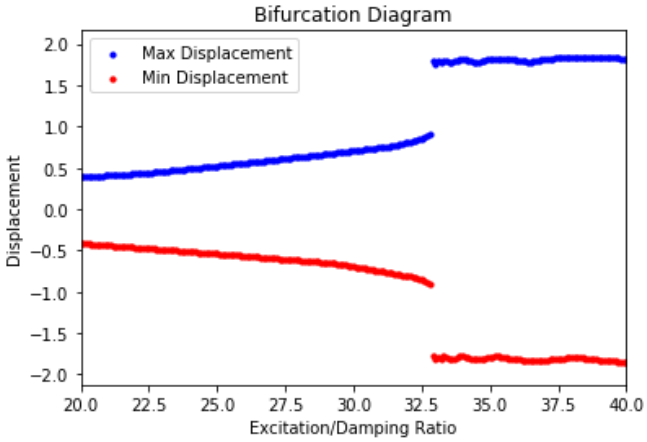

Figure 1. Bifurcation Plot

The plot is drawn from maximum and minimum displacement for each excitation amplitude to damping ratio. Clearly, as the ratio increases beyond around 33.0, the solution to the equation diverges. As in the logistic map, the curve would be seen as branching out in two directions; for simplicity of verification, the extrema of the displacements are marked. This is later confirmed from observing the phase space diagrams for various driving force values.

- Case 1: Free Motion

  $\delta = 0, \alpha = -1, \beta = 1, \gamma = 0, \omega = nonzero\ value$
  $\mathrm{x} = -1, \mathrm{v} = 1$

  Under absence of damping and excitation, the system remains to be in periodic oscillator motion, showing a closed curve attractor (limit cycle) in the phase space diagram. The fixed points (equilibrium) are located at three points, -1, 0, and 1, where 0 is the unstable one. This instability can be determined from the force curve (in red) where the slope is at the verge changing its sign; in the potential curve (in blue), the point at the origin can fall to either basin. The total energy, the sum of kinetic and potential, is conserved due to no dissipative or exciting forces applied to the system.

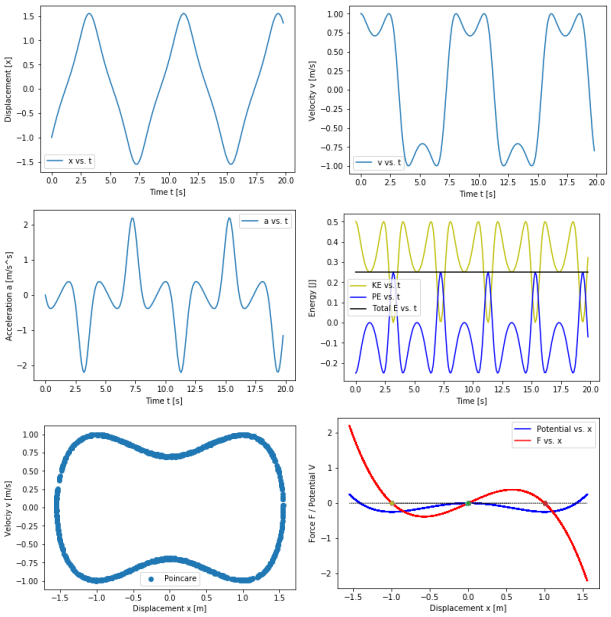

Figure 2. Case 1

- Case 2: Free Motion (different initial conditions)

$$\delta = 0, \alpha = -1, \beta = 1, \gamma = 0, \omega = nonzero\ value$$
$$x = -1.414, v = 0$$

With varied initial position, x, the system exhibits a slight change in the phase space diagram. The fixed point (equilibrium) is now located at x = -1 only, inducing the phase space diagram to look as such. The total energy is conserved still, with no dissipative or driven forces in place.

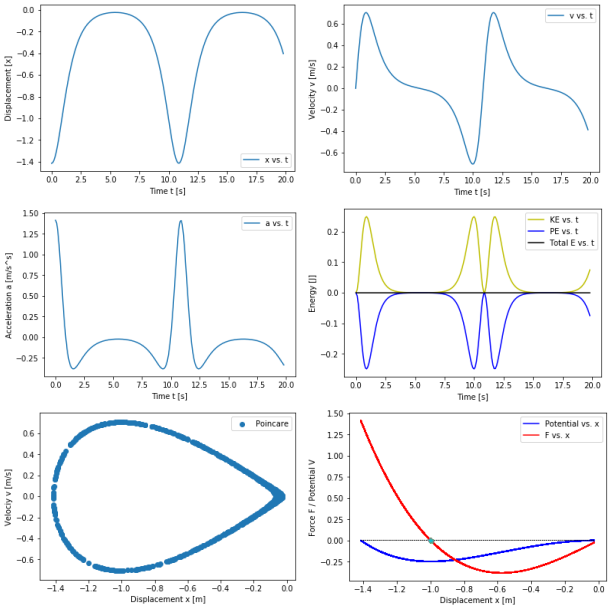

Figure 3. Case 2

- Case 3: Damped motion

$$\delta = 0.2, \alpha = -1, \beta = 1, \gamma = 0, \omega = nonzero\ value$$
$$x = -1.414, v = -1$$

Damping coefficient is slightly increased form Case 2, and the system becomes a dissipative one, as observable from the total energy dying away over time. There are fixed points at x = 1, and multiple experiments indicate that any initial conditions in this system lead to similar phase plot. The point to which the phase converges is the stable equilibrium point (attractor point).

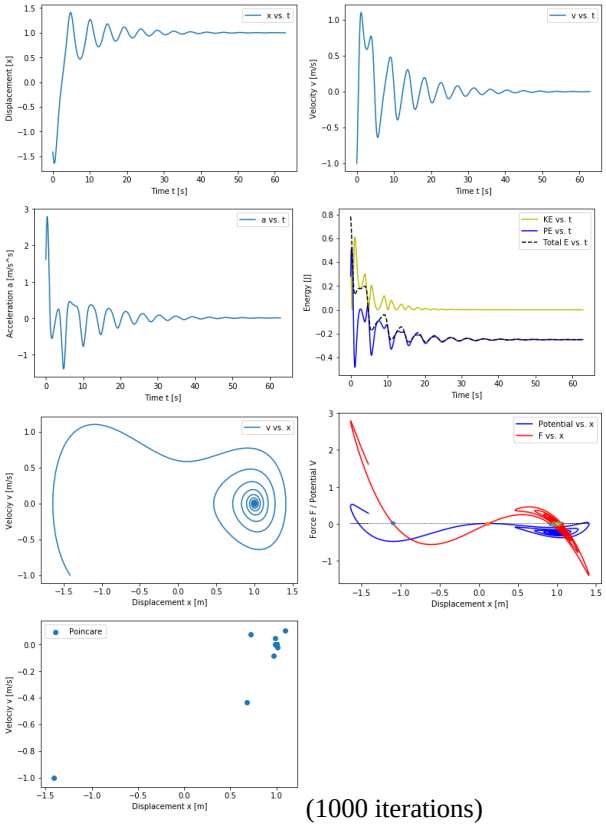

(1000 iterations)

Figure 4. Case 3

- Case 4: Damped driven motion

$$\delta = 0.1, \alpha = -1, \beta = 1, \gamma = 0.1, \omega = 1.4$$
$$x = 0, v = 0$$

As an external force is applied to the system, it increases the complexity of the phase plots. The motion of the mass observes a little bit of chaos and becomes no longer predictable, since any slight changes in the model parameters results in a very different movement of the particle. After initial transient state (aperiodic), it approaches a stable period around the fixed point at x=+1 in a closed orbit, exhibiting a limit cycle. At this point, the excitation is too weak to observe complete chaos.

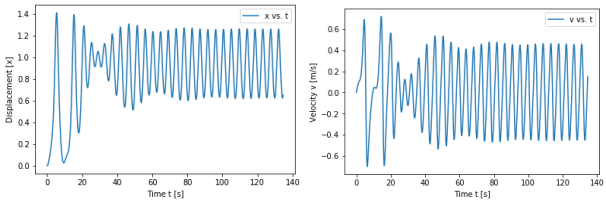

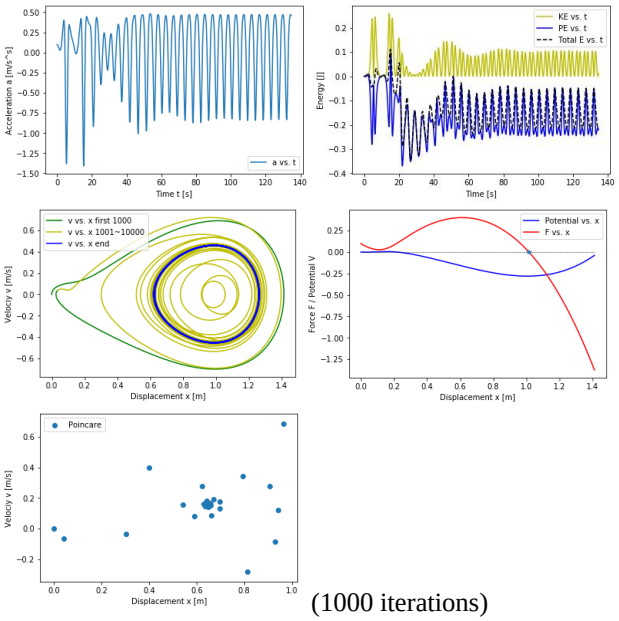

(1000 iterations)

Figure 5. Case 4

- Case 5: increased forcing exhibits three equilibrium fixed points, not yet chaotic;

$$\delta = 0.1, \alpha = -1, \beta = 1, \gamma = 0.32, \omega = 1.4$$
$$x = 0, v = 0$$

Increasing the driving force even further, multiple periodic orbits are observed; however, this is mainly due to initial transient period (in green). The mass seems to move in a haphazard manner between x = -1 and x = 1 fixed points, but after some time, it stabilizes in a periodic orbit, settling at x = -1 point. The decision of which fixed point it lands on depends primarily on the initial conditions and damping force. In addition, the displacement graph shows a period doubling effect: from ~ 4.48sec to ~9 sec after some transient state, with the period of the excitation determined from $T = \frac{2\pi}{\omega}$. This doubling causes bifurcation to take place.

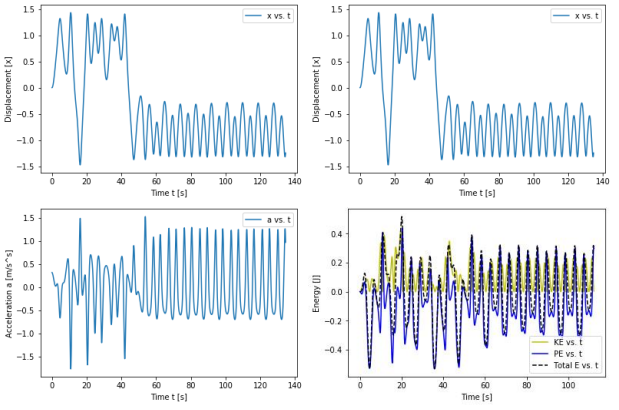

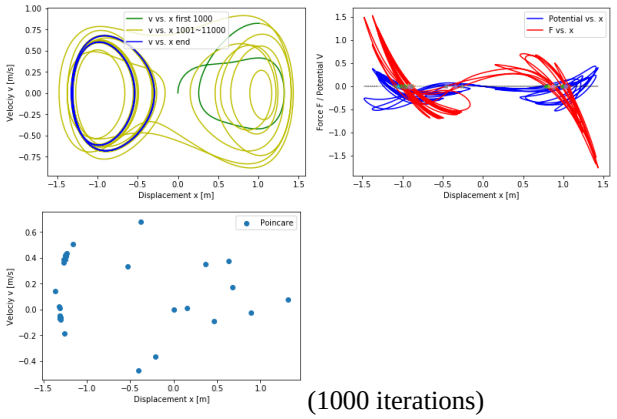

(1000 iterations)

Figure 6. Case 5

- Case 6: Damped Driven Motion (increased forcing even more ~0.34)

$$\delta = 0.1, \alpha = -1, \beta = 1, \gamma = 0.34, \omega = 1.4$$
$$x = 0, v = 0$$

As seen in the previous case, another period doubling occurs in the displacement graph. This time the phase space plot exhibits landing on a different fixed point, x = +1, as a result of slight increase in the applied force. However, the motion still settles in a periodic orbit after some initial transient state.

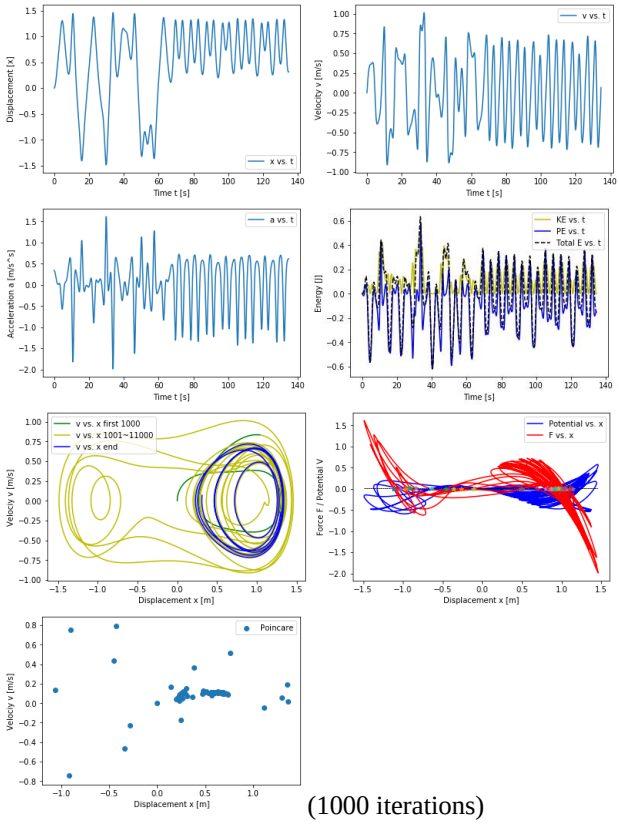

(1000 iterations)

Figure 7. Case 6

- Case 7: Damped Driven Motion (increased forcing even more ~0.38)

$$\delta = 0.1, \alpha = -1, \beta = 1, \gamma = 0.38, \omega = 1.4$$
$$x = 0, v = 0$$

Increasing the amplitude of excitation even further, a chaotic motion is finally observed from phase portrait. In all graphs plotted, periodic behavior is no longer exhibited throughout the iterations of time and space. It undergoes fixed points at x = -1, 0, +1 repeatedly without much pattern, and plotting 500 points at each period the Poincare graph for a general chaotic behavior is clearly noted. Varying initial conditions would cause the system to vary its trajectories in an unpredictable manner.

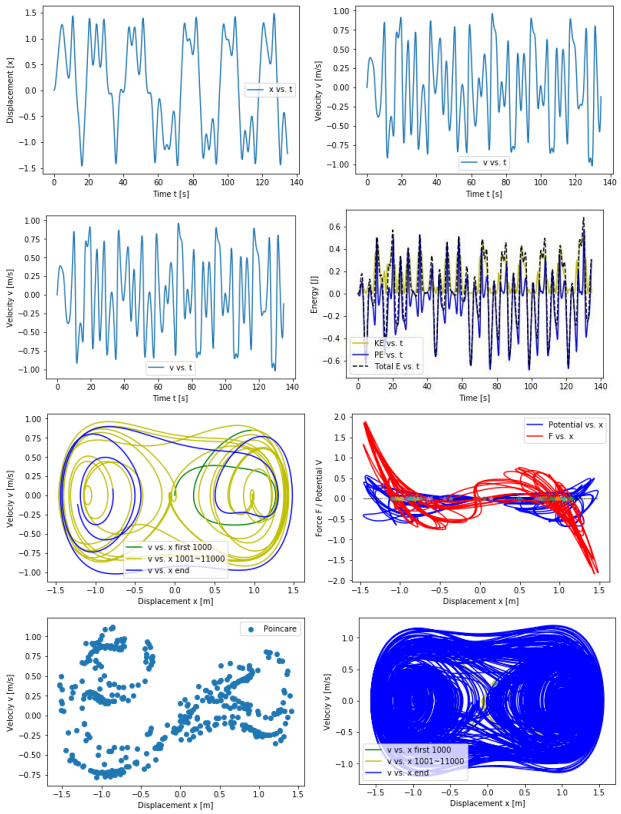

(500 iterations)

Figure 8. Case 7

Results - Poincare stroboscopic sections[4]

- Case 8: Period Doubling: more

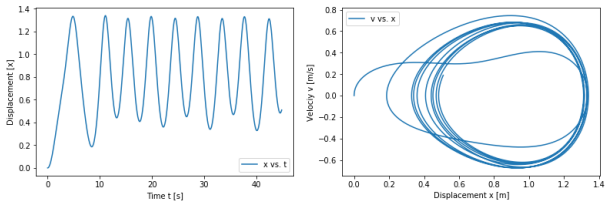

period: ~9sec, with delta=0.2

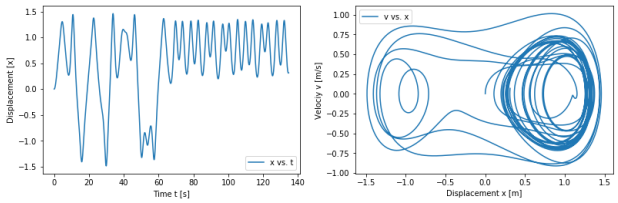

period: ~18sec, with delta=0.1

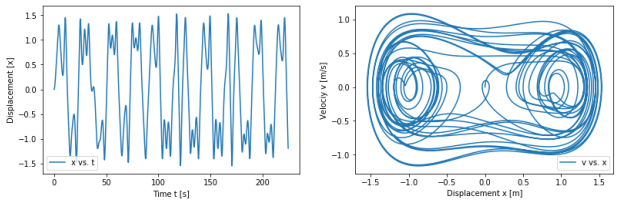

period:~36sec, with delta=0.09

Figure 9. Poincare Sections

As seen in multiple cases of parameters and initial condition settings, a slight change in the parameter values beyond some threshold induces a drastic change in the motion. Although the first two above exhibit some periodic state after initial transient state, further change no longer keeps such stable limit cycle, which is then chaotic.

Results - Frequency response

- Frequency response is obtained from the harmonic balance method, which is, simply put, with initial assumption of the solution as a linear combination of sinusoid performing transformation of variables to achieve an expression in terms of the relation of the sinusoid assumptions.

For the initial equations isolated to one side,

$$\ddot{x} + \delta\dot{x} + \alpha x + \beta x^3 - \gamma\cos(\omega t) = 0$$

for a solution of the form

$$x = z\cos(\omega t - \theta) = a\cos(\omega t) + b\sin(\omega t),$$

substitute $z^2 = a^2 + b^2$ *and* $\tan\theta = \frac{b}{a}$:

Then, $(-\omega^2 a + \omega\delta b + \alpha a + \frac{3}{4}\beta a^3 + \frac{3}{4}\beta a b^2 - \Upsilon)\cos(\omega t) + (-\omega^2 b + \omega\delta a + \frac{3}{4}\beta b^3 + \alpha b + \frac{3}{4}\beta b a^2)\sin(\omega t) + (\frac{1}{4}\beta a^3 - \frac{3}{4}\beta a b^2)\cos(3\omega t) + (\frac{3}{4}\beta b a^2 - \frac{1}{4}\beta b^3)\sin(3\omega t) = 0$

Neglecting super-harmonics at 3ω, and noting that cos(ωt) and sin(ωt) terms need to be zero,

$$(-\omega^2 a + \omega\delta b + \alpha a + \frac{3}{4}\beta a^3 + \frac{3}{4}\beta a b^2 - \Upsilon) = -\omega^2 b + \omega\delta a + \frac{3}{4}\beta b^3 + \alpha b + \frac{3}{4}\beta b a^2 = 0$$

Square both sides and isolate for Υ:

$$\therefore \quad \Upsilon^2 = [(\omega^2 - \alpha - \frac{3}{4}\beta z^2)^2 + (\delta\omega^2)^2]\, z^2$$

Frequency response plot is performed by plotting Υ/z against $\omega/\sqrt{\alpha}$.

(i) Hardening system

$\beta = 0.004 > 0$, $\delta = 0.1$, x = 0, v = 0, $\gamma = 1$, h = 0.1

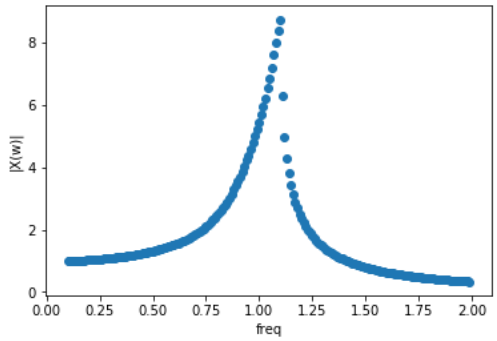

(ii) Softening System

β = -0.004 < 0

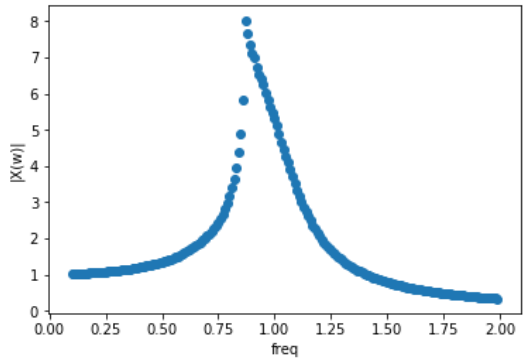

(iii) Linear system

β = 0

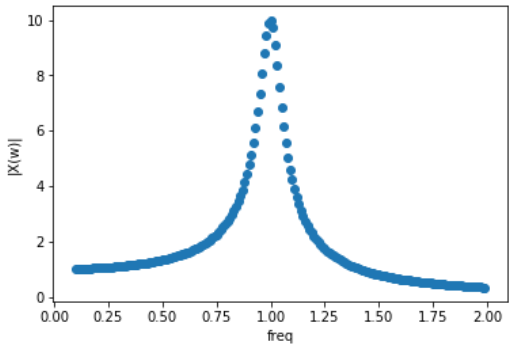

Figure 10. Frequency Responses (a), (b), (c), respectively

Depending on the value of nonlinearity coefficient, the system can be referred to as softening (β<0), linear(β=0), and hardening(β>0) system, as common for springs. When the nonlinearity parameter β is increased from zero, the frequency response curve bends to the left or the right depending on whether the system is softening or hardening, respectively. At the threshold value of |β|, the frequency response curve becomes multi-valued above certain frequency for a hardening system and below a certain frequency for a softening system. From experiments the threshold of the applied force amplitude required for a multi-valued frequency response curve can be determined, and hence "jump-up" and "jump-down" frequencies, and also the frequency at which this would occur[2].

Hysteresis effect is the dependence of the state in motion on the previous state. For the particular case above, the graphs are plotted in scatterplots such that the movement along one direction is visible; as a mass moves from the left for Fig. 10a, it follows up to the peak and falls directly down, while when it approaches from the right, it will not follow the path it came from. It will move towards left (lower excitation) through a different path at a lower magnitude response ('y' value). This asymmetric loop poses an interesting chaotic behavior on the system—bifurcation. As shown in phase space portraits in above figures, as the nonlinearity coefficient beta deviates from 0 (point of bifurcation), it is susceptible to chaotic behavior in motion[3].

Animation

The motions of the mass along single- and double-potential well are obtained by iterative animation plots in order to demonstrate a change in a single parameter set yields a completely different response in motion. The parameters are as shown below. With these parameters, phase space diagrams obtained from RK4-method and Python's built in function integrate.odeint in scipy library are compared.

For the following equation form

$$m\ddot{x} = -\delta\dot{x} - \alpha x - \beta x^3 + \gamma\cos(\omega t),$$

Table 2 Parameter Values for Videos

Parameter	Value	
	DoubleWell.mp4	SingleWell.mp4
mass, m	1	
damping, δ	**0**	**0.1**
stiffness, α	-1	
nonlinearity, β	1	
excitation, γ	0.05	
angular freq. ω	1.4	
step size, h	0.1	
Initial x	0	
Initial $\dot{x}$	0	

For single- and double-potential well,

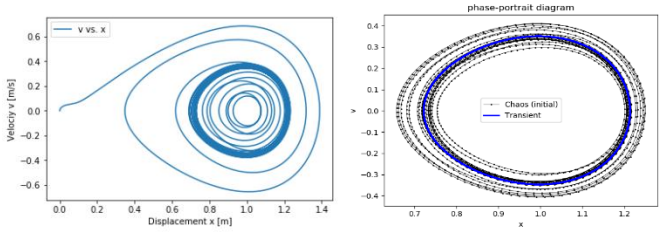

Figure 11(a), (b). Single-Potential Well Phase Portraits

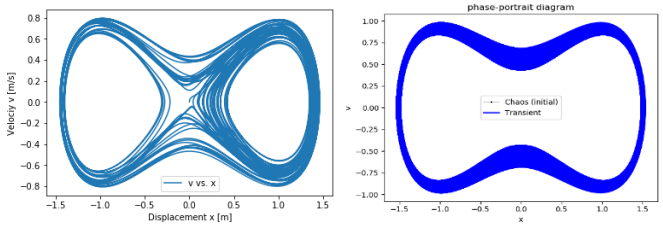

Figure 12(a), (b). Double-Potential Well Phase Portraits

Fig. 11(a) and 12(a) use fourth-order Runge-Kutta method to approximate the solutions x and ẋ, and 11(b) and 12(b) use LSODA algorithm, developed by Linda R. Petzold and Alan C. Hindmarsh from Livermore National Laboratory. This built-in algorithm for odeint library in Python an adaptive method for ordinary differential equations involving stiffness, using a dense or banded Jacobian for stiff systems while automatically selecting between non-stiff (Adams) and stiff (Backward Differentiation Formula) methods. The linear systems that arise are then solved by direct method (LU factor/solve)[14]. This originates from FORTRAN library, odepack, which solves a system of first order ordinary differential equations—the reason why this method is called twice for Duffing's Equation. Runge-Kutta solution phase portrait seems to have some points approaching the periodic state in the initial transient state, while the other seems to follow the periodic motion for the entire duration of time. This noticeable difference could be due to accuracy of the solutions; As the built-in method involves some degree of backward differentiattion method, which has lower order than Runge-Kutta (4th order), it seems intuitive that the former portrays trailing initial transient points in the plots.

In addition, from the RK4 approximated solution array in 1-D, a relatively simple visual python model is drawn. Since the case for nonlinearity parameter greater than zero is simply a spring, which is too common, the experiment is visualized for β<0.

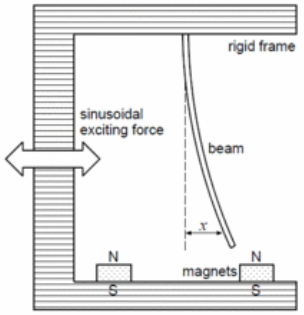

Figure 13(a). Moonbeam Visual Aid using VPython[11]

$x = 0, v = 0$
$\delta = 0.1, \alpha = -1, \beta = 1, \gamma = 0.38, \omega = 1.4, m = 1, h = 0.1$

sFor β<0 → a model of a periodically forced steel beam which is deflected toward the two magnets [10].
For β>0 → a forced oscillator model with a spring whose restoring force is written as $F = -\alpha x - \beta x^3$

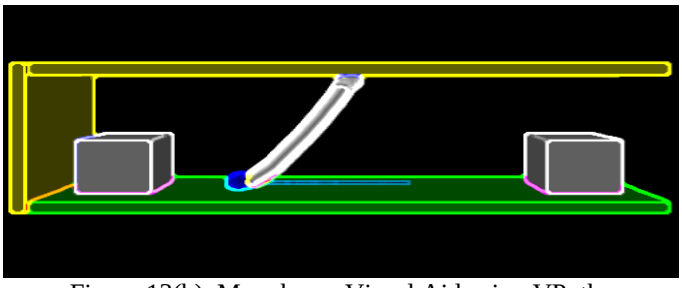

Figure 13(b). Moonbeam Visual Aid using VPython

Relevance to Course Materials

This pertains to the course topics in the sense that this deals with first numerically approximating the solution using a technique (Runge-Kutta algorithm) for an ordinary differential equation as well as verifying correct implementation, and visualization techniques including VPython (Visual Python) and animating objects over time to display time-iterated plots. Most importantly, analysis of chaotic behavior of a system via Poincare sections and periodic doubling observations from time and space series data is closely related to the course.

Conclusion

Through visualizing and analyzing a Duffing oscillator system under a number of initial and parameter conditions, the point at which chaos starts to be observed is approximately determined. Although the initial goals of applying the equation to the specific settings for a magnetoelastic beam deflected by magnets due to difficulty in determining the dynamics of the beam exactly, the characteristic behavior of such a system is closely examined in terms of its motion going through bifurcations. Poincare sections (phase-space diagrams) seemed to portray the nonlinear dynamics more evidently than expected; despite the need to iterate for multiples of periods for a complete points, it reveals a particular motion it is undergoing every period, leading to chaos. If more resources and time were allowed, it would be advisable to develop a equation specific to the Moonbeam structure, where magnetic, elastic, gravity forces could be taken into account to the steel beam deflected by two magnets, and also user-friendly interactive tool to tweak the parameter values and see the resulting graphs or motion.

References

[1] Beamer, K. J. (2013). Runge-Kutta - Numerical Solutions of Differential Equations. 1-16. doi:10.1002/9783527618774.ch2

[2] Brennan, M., Kovacic, I., Carrella, A., & Waters, T. (2008). On the jump-up and jump-down frequencies of the Duffing oscillator. Journal of Sound and Vibration, 318(4-5), 1250-1261. doi:10.1016/j.jsv.2008.04.032

[3] Das, S., Bhattacharyya, J., & Mohapatra, S. (2002). The Duffing Oscillator: A system with Cubic Nonlinearity. Retrieved April 1, 2019.

[4] Kovacic, I., & Brennan, M. (2011). The Duffing equation: Nonlinear oscillators and their behaviour. Oxford: Wiley.

[5] Marchionne, A., Ditlevsen, P., & Wieezorek, S. (2016). Three Types of Nonlinear Resonances. 1-17. Retrieved April 1, 2019.

[6] Moon, F., & Holmes, P. (1979). A magnetoelastic strange attractor. Journal of Sound and Vibration, 65(2), 275-296. doi:10.1016/0022-460x(79)90520-0

[7] Nayfeh, A. H., & Sanchez, N. E. (1989). Bifurcations in a forced softening duffing oscillator. International Journal of Non-Linear Mechanics, 24(6), 483-497. doi:10.1016/0020-7462(89)90014-0

[8] Oke, A. S. (2012). Numerical Computation of Lyapunov Exponents and Dimension in Nonlinear Dynamics and Chaos. 60-64. Retrieved April 1, 2019.

[9] Rand, R. H. (2003). Lecture Notes on Nonlinear Vibrations. 45, 13-13. Retrieved April 1, 2019, from *http://www.tam.cornell.edu/randdocs/*

[10] Kenfack, A. (2003). Bifurcation structure of two coupled periodically driven double-well Duffing oscillators. Chaos, Solitons & Fractals, 15(2), 205-218. doi:10.1016/s0960-0779(01)00250-8

[11] Wei, J., & Leng, G. (1997). Lyapunov exponent and chaos of Duffings equation perturbed by white noise. Applied Mathematics and Computation, 88(1), 77-93. doi:10.1016/s0096-3003(96)00307-4

[12] Zeni, A. R., & Gallas, J. A. (1995). Lyapunov exponents for a Duffing oscillator. Physica D: Nonlinear Phenomena, 89(1-2), 71-82. doi:10.1016/0167-2789(95)00215-4

[13] (Other) http://www.scholarpedia.org/article/Duffing_oscillator

[14] (Other) https://computation.llnl.gov/casc/odepack/